WOODY SAVANNAH TREE STRUCTURAL ASSESSMENT IN THE GREATER KRUGER NATIONAL PARK REGION, SOUTH AFRICA, USING MULTI-SEASONAL POLARIMETRIC SYNTHETIC APERTURE RADAR (SAR) AND OPTICAL DATA PRODUCT APPROACHES

Laven Naidoo[a], Renaud Mathieu[a], Moses Cho[a], Russell Main[a], Greg Asner[b]

[a]Ecosystem Earth Observation, Natural Resource and the Environment, CSIR, Pretoria, South Africa
Corresponding author contact details: LNaidoo@csir.co.za; (+27)12 841 2233

[b]Department of Global Ecology, Stanford University, Stanford, CA, USA

KEYWORDS: Polarimetry, SAR, optical, savannah, structure

ABSTRACT

With a mean net primary productivity of 7.2 tC/ha/year and a minimum woody coverage ranging from 10 to 30%, savannahs account for approximately 40% of the global carbon store. The savannah woody component impacts the fire regime, biomass production, nutrient cycling, soil erosion, the water cycle and the anthropogenic services (e.g. fuelwood provision) vital for the rural populace. The structural parameters which make up this vital woody component can be directly measured using active remote sensing sensors such as LiDAR and SAR due to their responsiveness to vegetative structure and high canopy penetration ability. The aim of this work is to model regional scale woody tree structural attributes [specifically woody canopy volume (CVOL), woody volume (TWV) and woody cover (TOT COV)] for the management of South African savannas. This goal was achieved by testing multiple dataset scenarios consisting of multi-seasonal and fully polarized RADARSAT-2 C-band satellite SAR data, airborne LiDAR derived tree structural metrics and Rapid Eye optical products in an integrated modelling approach. According to results, SAR data acquired in the middle of the dry season generated the best models in comparison to other seasons but ideally a dataset spanning all seasons were preferable to obtain the best modelled results (CVOL ~ R2 = 0.71; RMSE = 18487.0, SEP = 18947.2; TWV ~ R2 = 0.61, RMSE = 3797.7, SEP = 3936.9; TOT COV ~ R2 = 0.66, RMSE = 8.78, SEP = 8.94). HV and HH Polarized intensities was found to contribute the most to the overall success of the models with the woody canopy volume metric being predicted with the highest accuracies.

INTRODUCTION

Savannah woodlands (i.e. heterogeneous mixture of grass and woody plants) cover half of the African continent and occupy one fifth of the global land surface (Scholes and Walker, 1993). With a mean net primary productivity of 7.2 tC/ha/year and a minimum woody coverage ranging from 10 to 30%, savannahs account for approximately 40% of the global carbon store (House and Hall, 2001, cited in Collins et al, 2009). The savannah woody component impacts the fire regime, biomass production, nutrient cycling, soil erosion and the water cycle of these environments (Sankaran et al., 2008). From an anthropogenic point of view, the woody component provides numerous useful ecosystem resources such as fuelwood, construction timber and edible fruits (Shackleton et al.,

2007), which sustain the needs of the large rural populace in developing countries of Africa and regions of South Africa. The structural parameters which make up this vital woody component can be directly measured using available remote sensing sensors which can lead to future long term regional monitoring efforts.

Due to its responsiveness to vegetative structure, high canopy penetration ability and general weather independence, active remote sensing sensors such as LiDAR and SAR have been widely used for studying the woody component of trees (Popescu et al. 2011; Le Toan et al. 2011; Collins et al. 2009; Sun et al. 2011, Santoro et al. 2007). Studies, however, are under-represented in low woody density environments such as African savannahs (Mitchard et al. 2009; Ribeiro et al. 2008). The aim of this work is to model regional scale woody tree structural attributes [specifically woody canopy volume (CVOL), total woody volume (TWV) and total woody cover (TOT COV)] for the management of South African savannas. This aim is achieved by experimenting with multiple dataset scenarios consisting of multi-seasonal and fully polarized RADARSAT-2 C-band satellite SAR data, Rapid Eye optical products and airborne Carnegie Airborne Observatory (CAO) LiDAR data for validation, and implemented under an integrated modelling approach. The multi-seasonal nature of the SAR data allows for the sensing of the phenological related changes in canopy elements across three seasons – the end of the wet season (May-June 2009), middle of the dry season (August-September 2009) and the middle of the wet season (January-February 2010). The utilisation of fully polarized SAR data (HH, HV and VV) allows for the characterisation of the different tree scattering properties which is essential for building SAR related tree structure relationships. The use of Passive optical sensors alone has also played a role in accurately estimating tree structural parameters (Nichol and Sarker, 2011; Castillo-Santiago et al, 2010). This is made possible as tree structural characteristics (such as tree height, crown diameter etc.) can be measured from photo-interpretation and texture orientated modelling techniques (Lu et al., 2006). The red edge region (a dedicated band in the Rapid Eye sensor) has also been proven to be related to tree structure, health and leaf and canopy biophysical factors (Cho et al., 2012; Cho et al., 2008) and also played a role in estimating fresh and dry grass biomass (Cho et al., 2006). With this in mind, the main research questions to be answered in this study are:

1) Which season or combination of seasons are best for modelling savannah tree structural attributes using RADARSAT-2 C-band data? Which polarized intensity parameter(s) is/are the most influential?
2) How does the performance of multiple seasonal and polarized C-band SAR data compare with the use of optical product data alone in the modelling of tree structural parameters?

METHODOLOGY

Study Area:

The study area (figure 1) is the Southern Kruger National Park region which includes areas such as the Bushbuckridge communal rangelands (Justicea, Kildare, Argincourt and Xanthia informal settlement areas), the Skukuza region and the Sabi Sands Wildtuin. The study area is located in the Lowveld of the savannah biome in the north-eastern part of South Africa (31°00’ to 31°50’ Long E,

24°33’ to 25°00’ Lat S). These sites were selected to represent the different tree structural patterns associated with the different land management and disturbance regimes (ad hoc communal rangeland management versus park management), varying tree species composition (lowveld savanna and mixed forest fringe species) and geological substrates (granite and gabbro) present in the region.

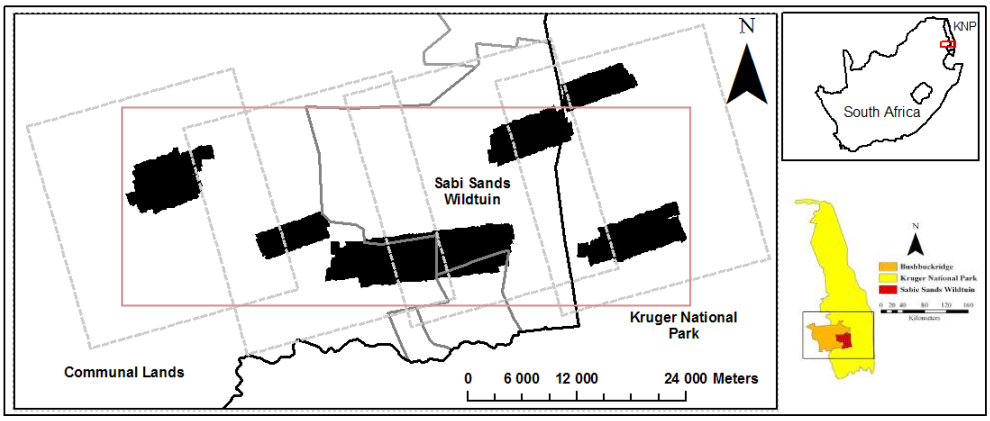

Figure 1: Map of the Southern Kruger National Park study region. The dotted grey line indicates the coverage of the RADARSAT-2 scenes while the solid red line indicates the coverage of the single Rapid Eye scene. The black shaded areas are the areas covered by the CAO LiDAR sensor.

Data Sources and Pre-processing:

The CAO LiDAR sensor (Asner et al, 2007), was flown in April/May 2008 across eight sites over the study area (figure 1). The wLiDAR subsystem operates with a laser emitting at 1064nm and was used in discrete-return mode (four ranges and four intensities per laser shot). Physical models of ground surfaces (Digital Elevation Model, DEM) and top-of-canopy surface models (CSM) were created by processing the raw LiDAR point clouds using the REALM (Optech Inc., Vaughn, Canada) and Terrascan / Terramatch (Terrasolid Ltd., Jyväskylä, Finland) software packages. Canopy height models (CHM, pixel size of 1.12 m) were computed by subtracting the DEM from the CSM. The raw point clouds were then further processed to produce pseudo waveforms, integrating 3D cloud points within a pixel of 5 x 5 m (Levick et al., 2009). These derived models and the pseudo waveforms were used to calculate the three LiDAR structural metrics used in this study. For the SAR data, C-band RADARSAT-2 Fine (4.7 x 5.1 m, range and azimuth nominal pixel spacing) Quad-Pol (C-HH, C-HV, C-VH, C-VV), Single Look Complex (SLC) images were acquired across three seasons (End of Wet, Middle of Dry and Middle of Wet) between May 2009 and February 2010. Amplitude and phase information was preserved in SLC products, and the data were calibrated. These seasons were chosen to best capture the typical phenological changes in savannah vegetation and the associated impacts on the SAR scattering interactions (e.g. moisture content). For the optical data, a single Rapid Eye image (for list of bands and overall data summary – refer to table 1) was acquired during April 2010 and was subjected to the atmospheric calibrations protocols. Additionally, three Normalized Vegetation Indices (NDVI, Green NDVI and mNDVI3) were calculated (table 1). These indices were assumed to provide an additional modelling predictor for estimating tree structural attributes. To avoid reliance on a particular NDVI index, all possible NDVI indices that could be calculated from the Rapid Eye band spectral coverage was used in the modelling analyses. All data

sources were then subset to present a common spatial coverage and were then stacked as a single layer in ENVI 4.7.

Table 1: Data sources used including associated description and time of acquisition

Sensor	Data Products	Spatial Resolution	Description	Date
Carnegie Airborne Observatory LiDAR	Total Woody Cover Metric (TOT COV) Total Woody Volume Metric (TWV) Total Canopy Volume Metric (CVOL) **[All metrics used as predicted variables / "ground truth"]**	1 m	Computed from Canopy Height Model (CHM) Computed from CHM and canopy cover Computed from the pseudo waveform as the sum of the within canopy hits at different heights above 0 m	April/May 2008
RADARSAT-2 C-Band	*Mean and Standard deviation of*: HH, HV and VV polarized products	5 m	Single Look Complex imagery	May-June 2009 (EWET) Aug-Sept 2009 (MDRY) Jan-Feb 2010 (MWET)
Rapid Eye	*Mean and Standard deviation of:* Blue Band (Band 1) Green Band (Band 2) Red Band (Band 3) Red Edge Band (Band 4) Near Infrared Band (Band 5) NDVI Green NDVI mNDVI3	5 m	Mean spectral reflectance and variance (Band 5 - Band 3)/(Band 5 + Band 3) [@] (Band 5 - Band 2)/(Band 5 + Band 2) [&] (Band 3 - Band 2)/(Band 3 + Band 2) [#]	April 2010

References: @ - Tucker (1979); & - Gitelson et al. (1996); # - Gandia et al. (2004)

Dataset Analysis:

A 105m grid vector layer was created and draped over the stacked layer products. The various variables (table 1) were integrated within this grid vector layer, from which mean and standard deviation were extracted. The grid size was found to be the best trade-off between the smallest mapping unit and relationship strength between the SAR and LiDAR dataset variables. The extracted information was used as the dependent (CVOL, TWV, TOT COV) and independent (HH, HV, VV and optical products) variables for the modelling analyses. It was assumed that the standard deviation would represent a simple 'textural' indicator which could be related to tree structure. The LiDAR dataset provided a very large and representative number of samples for model calibration and validation which would have not been possible to achieve at the ground level. Simple linear regression analyses were then performed between the optical products (independent variables) and the LiDAR structural metrics (dependent variables) to ascertain which optical products would be included into the optical-only model. This would reduce the chance of potential model over-fitting and improve computational performance.

For the modelling process, the SAR full polarimetry variables were grouped into six scenarios per season and three multi-seasonal scenarios while the important optical products were grouped together as a separate optical-only scenario. These scenarios were chosen to best explore the relationships between the SAR and the LiDAR structural metrics on the single and multi-seasonal basis and also explore the influence of the optical products alone on model performance. The datasets comprising of each of these scenarios were then fed into a bootstrapping stepwise multiple-linear regression algorithm (10% data split for training and 90% for validation). Model summary statistics such as coefficient of determination (R2), root mean square error (RMSE) and standard error of prediction (SEP), were produced to ascertain the best model and independent/predictor variables to be used.

RESULTS AND DISCUSSION

We first investigated the best optical products to use with the optical-only model. Figure 2 illustrated an overall low correlation between the 16 optical products and the LiDAR structural metrics which indicated a very minimally relation to general structural properties of trees. Mean GNDVI, mNDVI3 and NDVI indices and mean blue, green, red and red edge bands yielded relationships greater than 0.1 with the mean green band yielding the highest R2 of 0.25 for CVOL and total cover metrics. It was expected that these NDVI indices would be more correlated with the total cover metric as a higher NDVI measure with be related to a greater vegetative presence but this is not the case. The Near Infrared and all optical standard deviation counterparts yielded no relationships with the LiDAR metrics. All optical products were the least related to the TWV metric. Nevertheless, the seven optical products which displayed some degree of a relationship with the LiDAR metrics were included in the modelling process.

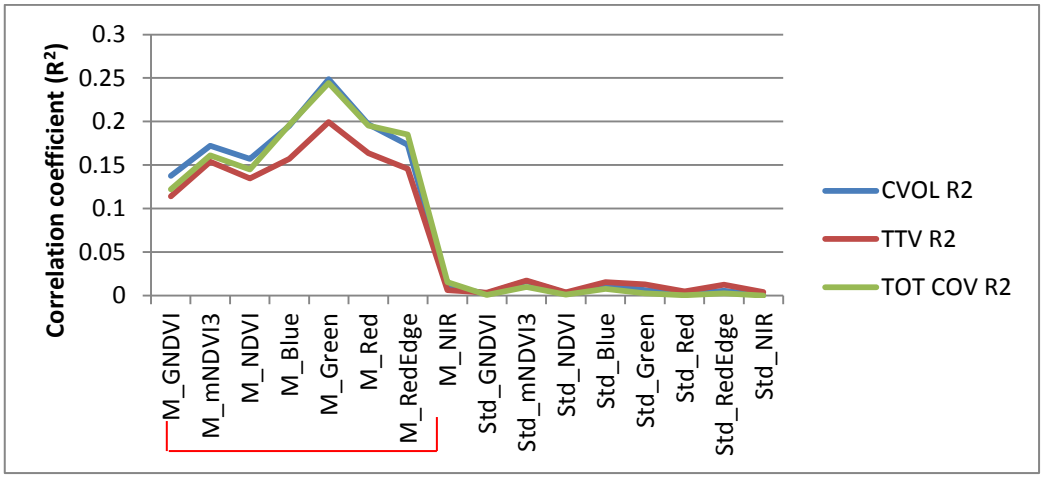

Figure 2: Correlation coefficients of 16 optical products correlated against the three LiDAR tree metrics (In the variable names, 'M' = Mean and 'Std' = Standard deviation)

Single and multi-seasonal modelled results for estimating the three LiDAR metrics (CVOL, TWV and TOT COV) were summarised in table 2. Considering all the individual and multi-seasonal scenario results, the woody Canopy Volume (CVOL) metric was the most accurately predicted with Total woody volume yielding the poorest results. On examination of the individual seasons, the middle of the dry season (MDRY) yielded the best modelled performance for the estimation of the LiDAR

metrics (CVOL ~ R2 = 0.66; RMSE = 19938.9, SEP = 20109.9; TWV ~ R2 = 0.57, RMSE = 3964.9, SEP = 3998.3; TOT COV ~ R2 = 0.61, RMSE = 9.36, SEP = 9.47). Since the majority of savanna trees have little or no leaves during the MDRY season more C-band SAR backscatter interactions with the branch elements within the canopy and the trunk itself may have occurred, which would have given better estimates of tree volumetric metrics. The end of the wet season (EWET) yielded the poorest model results, probably because this is a transition season when moisture conditions are the most variable in the landscape. When examining the historic rainfall data of the area (not shown in this paper), it was clear that particular heavy rainfall event may have marred the SAR acquisition in May 2009 (EWET). The best performing models (MDRY) comprised of the mean and standard deviation of all three SAR polarized intensities (HH, HV and VV) with HV polarized intensity, followed by HH, contributing most to the overall accuracies. This is consistent with results obtain by other studies in woodlands and savannahs for C-, L-, and P-band datasets (Collins et al. 2009; Lucas et al. 2006; Mitchard et al. 2009). Results improved even further when all available seasonal data (EWET, MDRY and MWET) of these three polarized intensities were utilised to create the best SAR-only model (CVOL ~ R2 = 0.71; RMSE = 18487.0, SEP = 18947.2; TWV ~ R2 = 0.61, RMSE = 3797.7, SEP = 3936.9; TOT COV ~ R2 = 0.66, RMSE = 8.78, SEP = 8.94).

When considering the influence of the optical data alone in the modelling process, results were poor with large RMSE and SEP values. In contrast to the SAR results, it seems that the optical products alone do not possess the information which sufficiently represents the tree structural variability evident in savanna environments. The next important step in this study would be the integration of the best performing optical and SAR variables into a single model to ascertain whether the fusion of optical and SAR data can improve the modelling of these tree structural metrics. Additionally, as a recommendation for further studies, other more structure oriented optical products such as image textures would need to be derived. Optical data acquired during a season where the grasses are dry and the trees are still green (e.g. spring) could also be useful as the optical indices will display ranges of values which could be more contrasting of the woody component while the textures of the grassy component will appear smooth. The exploration of other more robust statistical techniques such as Partial Least Square Regression (PLSR) and non-linear PLSR would be recommended as they are more suited to data displaying co-linearity and are more resilient towards model over-fitting.

CONCLUSION

After experimenting with the fusion of multi-seasonal C-band RADARSAT-2 data and Rapid Eye optical products for the modelling and prediction of tree structural metrics (CVOL, TTV and TOT COV) in South African savannahs, the following conclusions can be made: 1) SAR data acquired in the middle of the dry season generates the best models in comparison to other seasons but ideally a dataset spanning all seasons are preferable for best results; 2) HV and HH Polarized intensities contributed the most to the overall success of the models and 3) the CVOL metrics was predicted with the highest accuracies compared to the other metrics.

Table 2: Modelled results for CVOL, TTV and TOT COV across different single season and multi-seasonal data scenarios

Seasons	Variables selected by stepwise multiple linear regression	CVOL			TTV			TOT COV		
		M_R2	M_RMSE	M_SEP	M_R2	M_RMSE	M_SEP	M_R2	M_RMSE	M_SEP
EWET	HH MEAN, HH STDEV	0.25	29731.5	29943.1	0.19	5424.5	5430.9	0.24	13.09	13.11
	HV MEAN, HV STDEV	0.33	27885.7	28164.7	0.29	5090.1	5120.6	0.32	12.35	12.41
	VV MEAN, VV STDEV	0.22	30314.9	30517.3	0.18	5478.7	5499.8	0.20	13.33	13.47
	MEAN and STDEV of HH, HV	0.35	27686.7	27847.4	0.32	4987.5	5043.7	0.33	12.27	12.31
	MEAN and STDEV of HV, VV	0.37	27223.8	27480.3	0.30	5009.2	5064.6	0.35	12.05	12.17
	MEAN and STDEV of HH, HV, VV	0.39	26646.8	26972.7	0.34	4901.2	4918.8	0.37	11.91	12.07
MDRY	HH MEAN, HH STDEV	0.57	22424.0	22600.4	0.48	4349.8	4371.3	0.51	10.43	10.46
	HV MEAN, HV STDEV	0.63	20850.2	20950.0	0.54	4050.1	4057.1	0.58	9.69	9.76
	VV MEAN, VV STDEV	0.22	30286.1	30538.2	0.21	5363.3	5404.0	0.19	13.47	13.53
	MEAN and STDEV of HH, HV	0.65	20373.2	20627.3	0.56	3978.6	4038.7	0.59	9.58	9.67
	MEAN and STDEV of HV, VV	0.63	20701.6	20924.7	0.55	4009.5	4055.9	0.57	9.72	9.75
	MEAN and STDEV of HH, HV, VV	0.66	19938.9	20109.9	0.57	3964.9	3998.3	0.61	9.36	9.47
MWET	HH MEAN, HH STDEV	0.33	28095.4	28272.8	0.23	5291.6	5267.5	0.31	12.44	12.52
	HV MEAN, HV STDEV	0.36	27381.7	27684.5	0.27	5150.4	5182.2	0.33	12.16	12.28
	VV MEAN, VV STDEV	0.34	27772.9	27822.4	0.26	5148.3	5197.1	0.32	12.36	12.38
	MEAN and STDEV of HH, HV	0.37	27256.5	27414.9	0.28	5106.3	5136.1	0.34	12.12	12.18
	MEAN and STDEV of HV, VV	0.41	26301.4	26492.2	0.30	5054.7	5049.7	0.38	11.75	11.82
	MEAN and STDEV of HH, HV, VV	0.43	25997.7	26159.1	0.34	4906.7	4965.7	0.40	11.62	11.71
All Seasons	MEAN and STDEV of HH, HV and VV	0.71	18487.0	18947.2	0.61	3797.7	3936.9	0.66	8.78	8.94
Winter (MDRY) & Summer (MWET)	MEAN and STDEV of HH, HV, VV	0.71	18619.0	19015.7	0.59	3871.0	3932.4	0.65	8.85	9.00
Winter (MDRY) & Autumn (EWET)	MEAN and STDEV of HH, HV, VV	0.69	19050.6	19383.8	0.59	3860.9	3972.1	0.65	8.95	9.13
Single date acquisition	MEAN of GNDVI, mNDVI3, NDVI, Blue, Green, Red, Red Edge	0.54	26662.2	27177.6	0.47	5070.8	5157.0	0.54	11.2	11.5

ACKNOWLEDGEMENTS

The authors would like to thank the Council for Scientific and Industrial Research (CSIR) and the Department of Science and Technology, through the grant "Earth Observation Application Development in Support of the SA EO Strategy", for funding this study. The RADARSAT-2 scenes were provided by MacDonald Dettwiler and Associates Ltd. - Geospatial Services Inc. (MDA GSI), the Canadian Space Agency (CSA), and the Natural Resources Canada's Centre for Remote Sensing (CCRS) through the Science and Operational Applications Research program (SOAR). Thanks also go to the Andrew Mellon Foundation for the funding of the airborne remote sensing with the CAO. The CAO was made possible by the W.M. Keck Foundation, the Gordon and Betty Moore Foundation and William Hearst III. The hyperspectral and LiDAR pre-processed data products used in this study was made possible by the CAO team including T. Kennedy-Bowdoin, D. Knapp, J. Jacobson and R. Emerson. Finally, thanks also go the colleagues at the Earth Observation unit at the CSIR for their assistance and support.

REFERENCES

Asner, G.P., Knapp, D.E., Kennedy-Bowdoin, T., Jones, M.O., Martin, R.E., Boardman, J., Field, C.B., 2007. Carnegie Airborne Observatory: in-flight fusion of hyperspectral imaging and waveform light detection and ranging (wLiDAR) for three-dimensional studies of ecosystems. *Journal of Applied Remote Sensing*, 1

Castillo-Santiago, M.A., Ricker, M., de Jong, B.H.J., 2010. Estimation of tropical forest structure from SPOT-5 satellite images. *International Journal of Remote Sensing*, 31 (10), pp 2767-2782

Cho, M.A., Debba, P., Mutanga, O., Dudeni-Tlhone, N., Magadla, T., Khuluse, S.A., 2012. Potential utility of the spectral red-edge region of SumbandilaSat imagery for assessing indigenous forest structure and health. *International Journal of Applied Earth Observation and Geoinformation*, 16, pp 85-93

Cho, M.A., Skidmore, A.K., Atzberger, C., 2008. Towards red-edge positions less sensitive to canopy biophysical parameters for leaf chlorophyll estimation using properties optique spectrales des feuilles (PROSPECTS) and scattering by arbitrarily inclined leaves (SAILH) simulated data. *International Journal of Remote Sensing*, 29(8), pp 2241-2255

Cho, M.A., Sobhan, I.M., Skidmore, A.K., 2006. Estimating fresh grass/herb biomass from HYMAP data using the red-edge position. *Conference on Remote Sensing and Modelling of Ecosystems for Sustainability III*. *Proceedings of the Society of Phot-Optical Instrumentation Engineering*, 6298, pp 29805-29805

Collins, J.N., Hutley, L.B., Williams, R.J., Boggs, G., Bell, D., Bartolo, R., 2009. Estimating landscape-scale vegetation carbon stocks using airborne multi-frequency polarimetric synthetic aperture radar (SAR) in the savannahs of North Australia. *International Journal of Remote Sensing*, 30 (5), pp 1141-1159

Gandia, S., Fernández, G., García, J.C., Moreno, J., 2004. Retrieval of vegetation biophysical variables from CHRIS/PROBA data in the SPARC campaign. *ESA SP,* 578, pp 40–48.

Gitelson, A.A., Kaufman, Y.J., Merzlyak, M.N., 1996. Use of a green channel in remote sensing of global vegetation from EOS–MODIS. *Remote Sensing of Environment,* 58 (3), pp 289–298

Le Toan, T., Quegan, S., Davidson, M.W.J., Balzter, H., Paillou, P., Papathanassiou, K., Plummer, S., Rocca, F., Saatchi, S., Shugart, H., Ulander, L., 2011. The BIOMASS mission: Mapping global forest biomass to better understand the terrestrial carbon cycle. *Remote Sensing of Environment*, 115, pp 2850-2860

Levick, S.R., Asner, G.P., Kennedy-Bowdoin, T., & Knapp, D.E., 2009. The relative influence of fire and herbivory on savanna three-dimensional vegetation structure. *Biological Conservation, 142*, pp 1693-1700

Lu, D., 2006. The potential and challenge of remote sensing-based biomass estimation, *International Journal of Remote Sensing*, 27 (7), pp 1297-1328

Lucas, R.M., Cronin, N., Lee, A., Moghaddam, M., Witte, C., & Tickle, P., 2006. Empirical relationships between AIRSAR backscatter and LiDAR-derived forest biomass, queensland, Australia. *Remote Sensing of Environment*, 100, pp 407-425

Mitchard, E.T.A., Saatchi, S.S., Woodhouse, I.H., Nangendo, G., Ribeiro, N.S., Williams, M., Ryan, C.M., Lewis, S.L., Feldpausch, T.R., Meir, P., 2009. Using satellite radar backscatter to predict above-ground woody biomass: A consistent relationship across four different African landscapes. *Geophysical Research Letters*, 36, pp 1-6

Nichol, J.E., Sarker, L.R., 2011. Improved biomass estimation using the texture parameters of two high-resolution optical sensors. *IEEE Transactions on Geoscience and Remote Sensing*, 49 (3), pp 930-948

Popescu, S.C, Zhao, K., Neuenschwander, A., Lin C., 2011. Satellite LiDAR versus small footprint airborne LiDAR: comparing the accuracy of aboveground biomass estimates and forest structure metrics at footprint level. *Remote Sensing of Environment*, 115, pp 2786-2797

Ribeiro, N.S., Saatchi, S.S., Shugart, H.H., Washington-Allen, R.A., 2008. Aboveground biomass and Leaf Area Index (LAI) mapping for Niassa Reserve, northern Mozambique. *Journal of Geophysical Research-Biogeosciences*, 113, pp 12

Sankaran, M., Ratnam, J., Hanan, N., 2008. Woody cover in African savannas: the role of resources, fire and herbivory. *Global Ecology and Biogeography, 17*, pp 236-245

Santoro, M., Shvidenko, A., McCallum, I., Askne, J., Schmullius, C., 2007. Properties of ERS-1/2 coherence in the Siberian boreal forest and implications for stem volume retrieval. *Remote Sensing of Environment*, 106, pp 154-172

Scholes, R.J., Walker, B.H., 1993. An African Savanna: Synthesis of the Nylsvley Study. Cambridge: Cambridge University Press

Shackleton, C.M., Shackleton, S.E., Buiten, E., Bird, N., 2007. The importance of dry woodlands and forests in rural livelihoods and poverty alleviation in South Africa. *Forest Policy and Economics*, 9, pp 558-577

Sun, G., Jon Ranson, K., Guo, Z., Zhang, Z., Montesano, P., Kimes, D., 2011. Forest biomass mapping from LiDAR and Radar synergies. *Remote Sensing of Environment*, 115, pp 2906-2916

Tucker, C.J., 1979. Red and photographic infrared linear combinations for monitoring vegetation. *Remote Sensing of Environment,* 8 (2), pp 127–150.

Viergever, K.M., Woodhouse, I.H., Stuart, N., 2008. Monitoring the world's savanna biomass by earth observation. *Scottish Geographical Journal*, 124 (2-3), pp 218-225